MITSUBISHI ELECTRIC RESEARCH LABORATORIES
https://www.merl.com

Adaptive Observer-Based Detection of Inter-Turn Short-Circuit and Demagnetization Faults in Permanent Magnet Synchronous Motors

Yang, Ge; Wang, Yebin; Liu, Dehong; Lin, Chungwei; Wang, Bingnan

TR2026-158 October 29, 2026

Abstract

This paper presents an adaptive observer-based method for detecting inter-turn short-circuit (ITSC) and permanent-magnet (PM) demagnetization faults in permanent magnet synchronous motors (PMSMs). The effects of these faults are incorporated into the PMSM dq-frame current model, where the ITSC fault is represented by equivalent fault-current components and the demagnetization fault is reflected by a variation in the PM flux linkage. An adaptive observer, driven by measured dq-axis voltages, stator currents, and electrical speed, estimates the fault-current components and the PM flux linkage online. Two residuals are then constructed from the estimated fault-current magnitude and the deviation of the estimated flux linkage from its nominal value, enabling discrimination among ITSC, demagnetization, and combined-fault scenarios. MATLAB/Simulink studies under load disturbances, demagnetization, ITSC, and sequential combined faults validate the residual behavior and demonstrate robustness against non-fault load variations.

IEEE Industrial Electronics Society (IECON) 2026

© 2026 IEEE. Personal use of this material is permitted. Permission from IEEE must be obtained for all other uses, in any current or future media, including reprinting/republishing this material for advertising or promotional purposes, creating new collective works, for resale or redistribution to servers or lists, or reuse of any copyrighted component of this work in other works.

Mitsubishi Electric Research Laboratories, Inc.
201 Broadway, Cambridge, Massachusetts 02139

Adaptive Observer-Based Detection of Inter-Turn Short-Circuit and Demagnetization Faults in Permanent Magnet Synchronous Motors

Ge Yang
Department of Electrical Engineering
University at Buffalo
gyang22@buffalo.edu

Yebin Wang
Mitsubishi Electric Research Laboratories
Cambridge, USA
yebinwang@merl.com

Dehong Liu
Mitsubishi Electric Research Laboratories
Cambridge, USA
liudh@merl.com

Chungwei Lin
Mitsubishi Electric Research Laboratories
Cambridge, USA
clin@merl.com

Bingnan Wang
Mitsubishi Electric Research Laboratories
Cambridge, USA
bwang@merl.com

***Abstract*—This paper presents an adaptive observer-based method for detecting inter-turn short-circuit (ITSC) and permanent-magnet (PM) demagnetization faults in permanent magnet synchronous motors (PMSMs). The effects of these faults are incorporated into the PMSM dq-frame current model, where the ITSC fault is represented by equivalent fault-current components and the demagnetization fault is reflected by a variation in the PM flux linkage. An adaptive observer, driven by measured dq-axis voltages, stator currents, and electrical speed, estimates the fault-current components and the PM flux linkage online. Two residuals are then constructed from the estimated fault-current magnitude and the deviation of the estimated flux linkage from its nominal value, enabling discrimination among ITSC, demagnetization, and combined-fault scenarios. MATLAB/Simulink studies under load disturbances, demagnetization, ITSC, and sequential combined faults validate the residual behavior and demonstrate robustness against non-fault load variations.**

***Index Terms*—Permanent magnet synchronous motor, inter-turn short circuit, demagnetization, adaptive observer, fault detection.**

I. Introduction

Permanent magnet synchronous motors (PMSMs) have been widely used in electric vehicles, aerospace systems, industrial drives, and renewable-energy conversion systems due to their high power density, high efficiency, fast dynamic response, and compact structure [1]–[3]. As PMSMs are increasingly deployed in safety-critical and high-performance applications, reliable condition monitoring and fault detection have become essential for improving system availability and preventing unexpected failures. Among different fault types, inter-turn short-circuit (ITSC) faults and permanent-magnet demagnetization faults are particularly critical. ITSC faults can introduce circulating currents, localized thermal stress, and asymmetric magnetic fields, which may develop into severe winding failures [4], [5]. Demagnetization faults, on the other hand, reduce the effective permanent-magnet flux linkage and degrade torque production, efficiency, and control performance [6]. Therefore, accurate detection and discrimination of ITSC and demagnetization faults are important for reliable PMSM operation.

Model-free and data-driven methods have been widely investigated for ITSC and demagnetization fault detection in PMSMs, including machine-learning-based approaches [7]–[9]. These methods usually train detection models offline using measurement data collected under different operating and fault conditions, and then use selected fault-sensitive features for online diagnosis. Although good detection performance can be achieved with sufficient training data, their effectiveness strongly depends on dataset quality and coverage, which may be difficult to guarantee in practical motor drive systems. Negative-sequence-analysis-based methods have also been used for ITSC fault detection by extracting fault-sensitive negative-sequence current components [10], [11]. However, such methods can be sensitive to operating conditions, parameter variations, and measurement noise, and they are mainly developed for ITSC faults rather than demagnetization faults.

Alternatively, model-based detection methods using PMSM dynamic models and fault mechanisms have been studied for fault estimation and diagnosis. Observer-based and Kalman-filter-based approaches have been widely investigated for PMSM fault detection [12]–[14]. In [12], two adaptive observers are designed to estimate the fault current and detect ITSC faults in PMSMs. A Kalman filter is employed in [13] for ITSC fault detection, where the stator-current estimation error is used as the fault indicator. In [15], a sliding-mode observer is developed to detect demagnetization faults and sensor faults. However, most existing ITSC fault detection methods assume a constant permanent-magnet flux linkage and neglect demagnetization effects in the motor model. Consequently, the coupling between ITSC faults and demagnetization-induced flux variation remains insufficiently addressed.

This paper investigates the joint detection of ITSC and

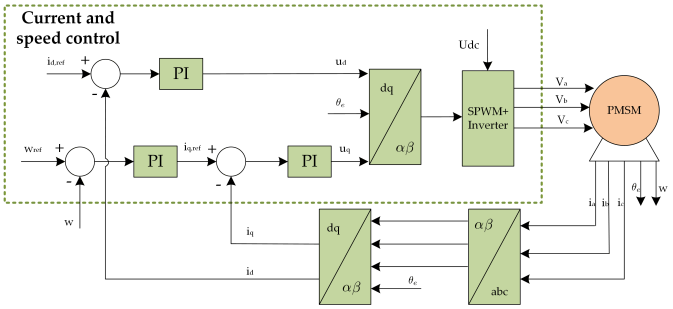

Fig. 1. PMSM drive system with field-oriented control.

demagnetization faults in PMSMs. Unlike many existing ITSC fault detection methods, which assume a constant permanent-magnet flux linkage and do not explicitly consider demagnetization effects, the proposed method incorporates both ITSC fault-current dynamics and permanent-magnet flux-linkage variation into the dq-frame current model. Based on this model, an adaptive observer is developed to estimate the equivalent dq-axis ITSC fault-current components and the PM flux linkage online. The estimated quantities are then used to construct residual indices for detecting and distinguishing ITSC faults, demagnetization faults, and their combined occurrence.

The rest of this paper is organized as follows. Section II introduces the PMSM model, the ITSC fault model, and the demagnetization fault model. Section III presents the proposed adaptive observer design for dual fault detection. Section IV provides simulation results to validate the effectiveness of the proposed method. Finally, Section V concludes the paper.

II. PMSM Modeling and Fault Analysis

A. PMSM Model Under Healthy Conditions

In this work, a PMSM driven by a three-phase voltage-source inverter is considered, as shown in Fig. 1. The motor drive adopts a cascaded PI-based field-oriented control (FOC) scheme similar to [16]. The measured three-phase currents are transformed into the synchronous d-q reference frame using the rotor electrical position. The rotor speed and position are assumed to be measurable. Under healthy operating conditions, the permanent-magnet flux linkage is aligned with the rotor d-axis and modeled as a constant scalar ψ_f. Therefore, the current dynamics in the synchronous d-q reference frame are expressed as

$$\begin{aligned} \dot{i}_d &= -\frac{R_s}{L_d} i_d + \frac{L_q}{L_d}\omega_e i_q + \frac{1}{L_d} u_d, \\ \dot{i}_q &= -\frac{R_s}{L_q} i_q - \frac{L_d}{L_q}\omega_e i_d + \frac{1}{L_q} u_q - \frac{\omega_e \psi_f}{L_q}. \end{aligned} \tag{1}$$

where i_d and i_q are the d- and q-axis stator currents, u_d and u_q are the corresponding stator voltages, R_s is the stator resistance, L_d and L_q are the d- and q-axis inductances, and ω_e is the electrical angular speed.

B. ITSC Fault and Demagnetization Fault Models

ITSC faults may occur in any stator phase. The shorted turns introduce an additional fault current, which affects the stator current dynamics through equivalent fault components in the synchronous dq reference frame. Demagnetization faults are mainly caused by irreversible degradation of the permanent magnets due to high temperature, excessive armature reaction, or aging [6]. Under uniform demagnetization, the permanent-magnet flux linkage is reduced from its nominal value. Let $\delta \in [0, 1)$ denote the demagnetization ratio. Then the faulty permanent-magnet flux linkage can be written as $\psi_f^* = (1 - \delta)\psi_f$, where ψ_f is the nominal permanent-magnet flux linkage. A larger value of δ represents a more severe demagnetization fault. Following the equivalent dq-axis ITSC representation in [17], i_{fd} and i_{fq} are defined as the equivalent d- and q-axis fault current, respectively. Considering both ITSC and demagnetization faults, the faulty dq-axis current dynamics of the PMSM can be written as

$$\begin{aligned} \frac{di_d}{dt} &= \frac{u_d}{L_d} - \frac{R_s}{L_d} i_d + \frac{R_s}{L_d} i_{fd} + \frac{\omega_e L_q}{L_d} i_q, \\ \frac{di_q}{dt} &= \frac{u_q}{L_q} - \frac{R_s}{L_q} i_q + \frac{R_s}{L_q} i_{fq} - \frac{\omega_e L_d}{L_q} i_d - \frac{\omega_e}{L_q}(1 - \delta)\psi_f. \end{aligned} \tag{2}$$

Compared with the healthy model, the ITSC fault introduces additional d- and q-axis fault-current terms, while the demagnetization fault reduces the effective PM flux linkage.

III. Adaptive Observer-Based Fault Detection Method

In this section, an adaptive observer-based fault detection framework is developed using the dq-frame PMSM current model. Although current-reference comparison may indicate an ITSC, the error is affected by operating conditions and controller action [18]. The proposed observer estimates both the ITSC-induced current perturbation and the demagnetization-induced flux-linkage change. The overall detection procedure is shown in Fig. 2. In existing ITSC detection methods [10], [12], the permanent-magnet flux linkage is assumed to remain constant, and demagnetization faults are not explicitly considered. However, when ITSC and demagnetization faults coexist, the flux variation caused by demagnetization can affect the current dynamics and may degrade fault detection performance. To address this issue, the proposed observer incorporates the demagnetization-induced flux variation into the fault detection framework. Using the generated residual signals, both ITSC and demagnetization faults can be detected.

A. Adaptive Observer Design

To detect ITSC and demagnetization faults in PMSMs, an augmented adaptive observer is developed in the dq synchronous reference frame. The measured stator currents i_d and i_q are used as the observer outputs, while the stator voltages u_d and u_q and the electrical angular speed ω_e are assumed to be available from the motor drive system. In the proposed observer, the effect of an ITSC fault is represented by two equivalent fault-current states, i_{fd} and i_{fq}, in the dq frame.

These augmented states describe the additional current components induced by shorted turns. In contrast, demagnetization mainly appears as a variation in the permanent-magnet flux linkage ψ_f. Therefore, estimating i_{fd}, i_{fq}, and ψ_f provides useful information for identifying and distinguishing ITSC and demagnetization faults. The estimated augmented state vector is defined as $\hat{x} = [\hat{i}_d \ \hat{i}_q \ \hat{\psi}_f \ \hat{i}_{fd} \ \hat{i}_{fq}]^T$. The current estimation errors are defined as $e_d = i_d - \hat{i}_d$, and $e_q = i_q - \hat{i}_q$. The current observer is designed as

$$\begin{aligned}\dot{\hat{i}}_d &= -\frac{R_s}{L_d}\left(\hat{i}_d - \hat{i}_{fd}\right) + \frac{\omega_e L_q}{L_d}\hat{i}_q + \frac{1}{L_d}u_d + l_d e_d,\\ \dot{\hat{i}}_q &= -\frac{R_s}{L_q}\left(\hat{i}_q - \hat{i}_{fq}\right) - \frac{\omega_e}{L_q}\left(L_d\hat{i}_d + \hat{\psi}_f\right) + \frac{1}{L_q}u_q + l_q e_q.\end{aligned} \tag{3}$$

The adaptive laws for the equivalent ITSC fault-current estimates are given by

$$\begin{aligned}\dot{\hat{i}}_{fd} &= -a_f\hat{i}_{fd} + g_d e_d,\\ \dot{\hat{i}}_{fq} &= -a_f\hat{i}_{fq} + g_q e_q,\end{aligned} \tag{4}$$

where l_d and l_q are the current observer gains, g_d and g_q are the adaptive gains for equivalent ITSC fault-current estimation, and $a_f > 0$ is a leakage coefficient introduced to improve the boundedness and robustness of the fault-current estimates.

The permanent-magnet flux linkage is updated using the following leakage-modified adaptation law:

$$\dot{\hat{\psi}}_f = -\gamma_\psi\frac{\omega_e}{L_q}e_q - a_\psi(\hat{\psi}_f - \psi_{f0}), \tag{5}$$

where $\gamma_\psi > 0$ is the flux adaptation gain, $a_\psi > 0$ is the leakage coefficient, and ψ_{f0} denotes the nominal healthy PM flux linkage. Since the q-axis current dynamics are directly affected by the permanent-magnet flux linkage, the q-axis current estimation error is used to adaptively estimate ψ_f. The observer gains are selected such that the current estimation errors are driven to a bounded neighborhood of zero under normal operation, while the adaptive states track the fault-related variations.

B. Fault Estimation and Detection Logic

Based on the augmented observer, two fault indicators are constructed for ITSC and demagnetization fault detection. The ITSC fault indicator is defined as the magnitude of the estimated equivalent fault-current vector:

$$r_{\mathrm{ITSC}} = \sqrt{\hat{i}_{fd}^2 + \hat{i}_{fq}^2}. \tag{6}$$

A larger value of r_{ITSC} indicates stronger shorted-turn-induced current components in the stator windings. Under healthy conditions, $\hat{i}_{fd}$ and $\hat{i}_{fq}$ remain close to zero. Once an ITSC fault occurs, the equivalent fault-current estimates increase and can indicate the fault severity.

The demagnetization fault indicator is defined as the deviation of the estimated permanent-magnet flux linkage from its nominal value:

$$r_{\mathrm{demag}} = \psi_{f0} - \hat{\psi}_f, \tag{7}$$

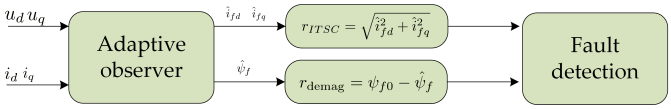

Fig. 2. Fault detection procedure.

where ψ_{f0} is the nominal permanent-magnet flux linkage. A positive increase in r_{demag} indicates a reduction in the magnet flux linkage, which corresponds to demagnetization. The fault decision logic is then given by

$$\begin{cases} r_{\mathrm{ITSC}} > T_{\mathrm{ITSC}} & \text{ITSC fault detected} \\ r_{\mathrm{demag}} > T_{\mathrm{demag}} & \text{demagnetization fault detected} \end{cases} \tag{8}$$

where T_{ITSC} and T_{demag} are predefined detection thresholds. These thresholds can be selected based on healthy-condition simulations or experiments by considering measurement noise, parameter uncertainty, and load/speed transients. The proposed method uses the adaptive observer not only to generate current estimation errors, but also to estimate physically meaningful fault-related quantities. Therefore, ITSC and demagnetization faults can be detected and distinguished based on their different effects on the equivalent fault-current states and the permanent-magnet flux linkage.

C. Stability Analysis

The stability of the proposed adaptive observer is analyzed using a Lyapunov-based approach. The PMSM model with ITSC and demagnetization effects can be written as

$$\dot{x} = Ax + Bu + Df_a + E\psi_f, \tag{9}$$

where $x = [i_d \ \ i_q]^T$, $u = [u_d \ \ u_q]^T$, and $f_a = [i_{fd} \ \ i_{fq}]^T$. The system matrices are expressed as

$$\begin{aligned} A &= \begin{bmatrix} -\dfrac{R_s}{L_d} & \dfrac{\omega_e L_q}{L_d} \\ -\dfrac{\omega_e L_d}{L_q} & -\dfrac{R_s}{L_q} \end{bmatrix}, \quad B = \begin{bmatrix} \dfrac{1}{L_d} & 0 \\ 0 & \dfrac{1}{L_q} \end{bmatrix}, \\ E &= \begin{bmatrix} 0 \\ -\dfrac{\omega_e}{L_q} \end{bmatrix}, \qquad D = \begin{bmatrix} \dfrac{R_s}{L_d} & 0 \\ 0 & \dfrac{R_s}{L_q} \end{bmatrix}. \end{aligned} \tag{10}$$

The designed observer model can be rewritten as

$$\dot{\hat{x}} = A\hat{x} + Bu + D\hat{f}_a + E\hat{\psi}_f + L(x - \hat{x}), \tag{11}$$

$$\dot{\hat{f}}_a = -a_f\hat{f}_a + G(x - \hat{x}), \tag{12}$$

$$\dot{\hat{\psi}}_f = \gamma_\psi E^T(x - \hat{x}) - a_\psi(\hat{\psi}_f - \psi_{f0}), \tag{13}$$

where $L = \mathrm{diag}(l_d, l_q)$ is the observer gain matrix, $G = \mathrm{diag}(g_d, g_q)$ is the adaptive gain matrix for fault-current estimation, $a_f > 0$ is the fault-current leakage coefficient, $\gamma_\psi > 0$ is the flux adaptation gain, $a_\psi > 0$ is the flux leakage coefficient, and ψ_{f0} is the nominal healthy PM flux linkage. Define the estimation errors as

$$e = x - \hat{x}, \qquad \tilde{f}_a = f_a - \hat{f}_a, \qquad \tilde{\psi}_f = \psi_f - \hat{\psi}_f. \tag{14}$$

Then, the error dynamics are obtained as

$$\dot{e} = (A - L)e + D\tilde{f}_a + E\tilde{\psi}_f, \tag{15}$$

$$\dot{\tilde{f}}_a = -a_f\tilde{f}_a - Ge + \dot{f}_a + a_f f_a, \tag{16}$$

$$\dot{\tilde{\psi}}_f = -a_\psi\tilde{\psi}_f - \gamma_\psi E^T e + \dot{\psi}_f + a_\psi(\psi_f - \psi_{f0}). \tag{17}$$

Similar to the bounded-fault assumption used in adaptive fault estimation [17], the following assumption is introduced.

Assumption 1: The equivalent ITSC fault current f_a, its derivative $\dot{f}_a$, the PM flux linkage ψ_f, and its variation $\dot{\psi}_f$ are bounded.

Choose the Lyapunov function candidate as

$$V = e^T Pe + \tilde{f}_a^T\tilde{f}_a + \tilde{\psi}_f^2, \tag{18}$$

where $P = P^T > 0$. Taking the time derivative of (18) yields

$$\begin{aligned}\dot{V} = {} & e^T\Pi e + 2e^T(PD - G^T)\tilde{f}_a + 2e^T(PE - \gamma_\psi E)\tilde{\psi}_f \\ & - 2a_f\tilde{f}_a^T\tilde{f}_a - 2a_\psi\tilde{\psi}_f^2 + 2\tilde{f}_a^T\dot{f}_a + 2a_f\tilde{f}_a^T f_a \\ & + 2\tilde{\psi}_f\dot{\psi}_f + 2a_\psi\tilde{\psi}_f(\psi_f - \psi_{f0}),\end{aligned} \tag{19}$$

where $\Pi = (A - L)^T P + P(A - L)$. By applying Young's inequality to the cross terms in (19), $\dot{V}$ is upper bounded as

$$\dot{V} \le e^T Me + \alpha_f\tilde{f}_a^T\tilde{f}_a + \alpha_\psi\tilde{\psi}_f^2 + \omega, \tag{20}$$

where

$$M = \Pi + \rho_1^2 WW^T + \rho_2^2 HH^T, \tag{21}$$

$$\alpha_f = -2a_f + \frac{1}{\rho_1^2} + \rho_3^2 + \rho_4^2, \tag{22}$$

$$\alpha_\psi = -2a_\psi + \frac{1}{\rho_2^2} + \rho_5^2 + a_\psi\rho_6^2, \tag{23}$$

where $\rho_i > 0$ $(i = 1, \ldots, 6)$ are positive constants introduced by Young's inequality, with $W = PD - G^T$ and $H = PE - \gamma_\psi E$. The bounded term is expressed as

$$\omega = \frac{1}{\rho_3^2}\dot{f}_a^T\dot{f}_a + \frac{a_f^2}{\rho_4^2}f_a^T f_a + \frac{1}{\rho_5^2}\dot{\psi}_f^2 + \frac{a_\psi}{\rho_6^2}(\psi_f - \psi_{f0})^2. \tag{24}$$

From Assumption 1, ω is bounded. Therefore, there exists a positive constant $\bar{\omega}$ such that $\omega \le \bar{\omega}$. Define the augmented estimation error vector as $\xi^T = \begin{bmatrix} e^T & \tilde{f}_a^T & \tilde{\psi}_f \end{bmatrix}$. Then (20) can be written as $\dot{V} \le \xi^T\Phi\xi + \bar{\omega}$, where

$$\Phi = \begin{bmatrix} M & 0 & 0 \\ 0 & \alpha_f I_2 & 0 \\ 0 & 0 & \alpha_\psi \end{bmatrix}. \tag{25}$$

If the observer gains and adaptation parameters are selected such that there exists a scalar $\lambda > 0$ satisfying $\Phi \le -\lambda I$, then $\dot{V} \le -\lambda\|\xi\|^2 + \bar{\omega}$. Thus, when

$$\|\xi\| > \sqrt{\frac{\bar{\omega}}{\lambda}}, \tag{26}$$

it follows that $\dot{V} < 0$. Hence, the current-estimation error, equivalent ITSC fault-current estimation error, and PM flux-linkage estimation error are uniformly ultimately bounded. As a result, $\hat{f}_a$ and $\hat{\psi}_f$ remain bounded, and the indicators $r_{\mathrm{ITSC}} = \|\hat{f}_a\|$ and $r_{\mathrm{demag}} = \psi_{f0} - \hat{\psi}_f$ provide bounded diagnostic measures of ITSC severity and PM flux reduction.

TABLE I
SIMULATION PARAMETERS

Parameter	Value
Pole pairs, p_m	2
Rated speed (rad/s)	314
Armature resistance, R_s (Ω)	0.605
d-axis inductance, L_d (mH)	12.65
q-axis inductance, L_q (mH)	12.65
Flux linkage, ψ_n (Wb)	0.83

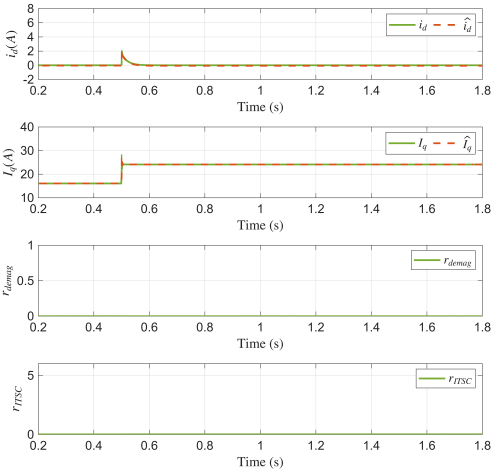

Fig. 3. Simulation results under load change at $t = 0.5$ s.

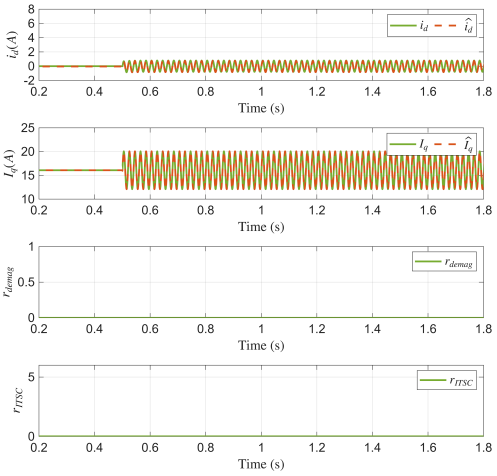

Fig. 4. Simulation results under unbalanced load change at $t = 0.5$ s.

IV. SIMULATION VERIFICATION

To verify the proposed observer-based demagnetization and ITSC fault detection framework, the PMSM drive system in Fig. 1 was modeled in MATLAB/Simulink. The simulation was conducted with a sampling time of $T_s = 5$ μs. The measured three-phase stator currents are transformed into the rotating d-q reference frame and used by the observer to estimate the corresponding current components. The residual signals are then generated from the observer and used for demagnetization and ITSC fault detection. The PMSM drive adopts a field-oriented control structure. The outer speed loop

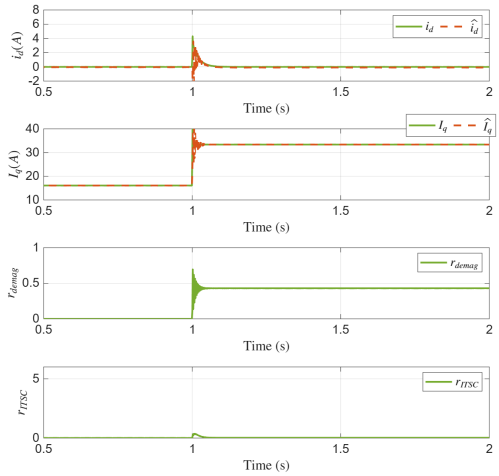

Fig. 5. Simulation results under a demagnetization fault introduced at $t = 1$ s, with the PM flux linkage decreased from 0.83 Wb to 0.6 Wb.

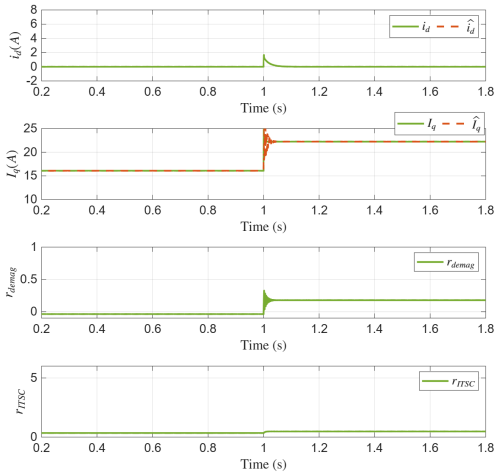

Fig. 6. Simulation results under a demagnetization fault with the PM flux linkage decreased from 0.83 Wb to 0.6 Wb at $t = 1$ s, with R_s increased by 10% and L_d and L_q increased by 5%.

generates the q-axis current reference, while the inner current loops regulate the d- and q-axis currents. The reference motor speed and reference i_d current are set to 314 rad/s and 0 A. The main simulation parameters are provided in Table I. The voltage commands are transformed to the stationary reference frame and applied to the PWM generator to drive the inverter. The currents are transformed into the d-q frame and provided to the observer for residual generation. The residuals r_{demag} and r_{ITSC} are used to distinguish different fault conditions.

A. Verification Under Non-Fault Disturbances

Before evaluating the fault detection performance, the robustness of the proposed method is tested under normal load-torque variation and an unbalanced load condition. In both cases, the load disturbance is introduced at $t = 0.5$ s. For the normal load-torque variation, the q-axis current changes according to the required electromagnetic torque, while the d-axis current remains close to its reference value after a short transient, as shown in Fig. 3. Although the operating point of the motor changes, both the demagnetization residual r_{demag} and the ITSC residual r_{ITSC} remain close to zero. This indicates that the proposed residual generation method does not misinterpret normal load variation as a motor fault. For the unbalanced load condition, oscillatory components appear in the d- and q-axis currents, as shown in Fig. 4. Nevertheless, both residual indicators remain bounded near zero, and no fault alarm is generated. Therefore, the proposed method is robust against load imbalance and can avoid false alarms caused by non-fault disturbances.

B. Verification Under Fault Conditions

The proposed method is further evaluated under demagnetization and ITSC fault scenarios. In the demagnetization fault case, the fault is introduced at $t = 1$ s. As shown in Fig. 5, after the fault occurs, the demagnetization residual r_{demag} increases significantly, while the ITSC residual r_{ITSC} remains close to zero. This result shows that the proposed method can correctly identify demagnetization faults without incorrectly classifying them as ITSC faults. To evaluate robustness against parameter uncertainty, R_s is increased by 10% and L_d and L_q by 5% from the values in Table I, while the observer parameters and gains remain unchanged. A demagnetization fault is introduced at $t = 1$ s. As shown in Fig. 6, the parameter mismatch causes small deviations in the residuals, while r_{demag} still increases after the demagnetization fault. These results demonstrate the robustness of the observer to the considered parameter variations. In the ITSC fault case, the fault is introduced at $t = 1$ s. As shown in Fig. 7, after the fault occurs, the current estimation error increases, and the ITSC residual r_{ITSC} rises clearly from its healthy-state value. In addition, r_{demag} also changes due to the coupling between the ITSC fault and the motor current dynamics. Compared with the demagnetization case, the ITSC fault produces a distinct residual pattern, which enables fault-type discrimination.

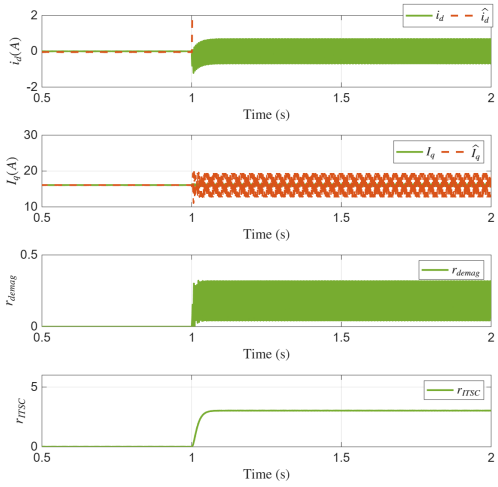

Fig. 7. Simulation results under an ITSC fault with a shorted-turn ratio of 0.02, introduced at $t = 1$ s.

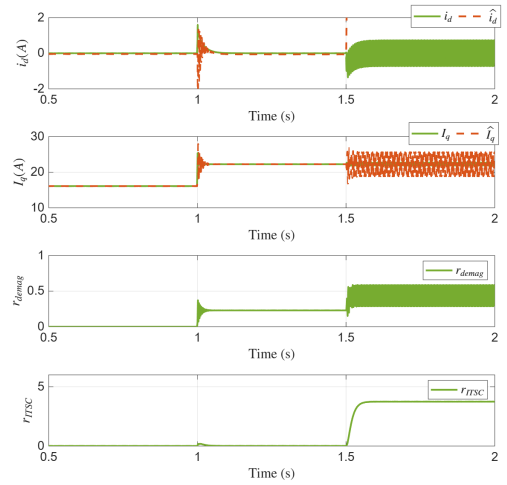

Fig. 8. Simulation results under sequential demagnetization and ITSC faults. The PM flux linkage is decreased from 0.83 Wb to 0.6 Wb at $t = 1$ s, followed by an ITSC fault with a shorted-turn ratio of 0.025 at $t = 1.5$ s.

Finally, a combined fault case is simulated, where a demagnetization fault is introduced at $t = 1$ s followed by an ITSC fault at $t = 1.5$ s. As shown in Fig. 8, after the demagnetization fault occurs, r_{demag} increases while r_{ITSC} remains near zero. When the ITSC fault is introduced, r_{ITSC} increases distinctly, while r_{demag} remains elevated. The sequential changes in the residuals demonstrate that the proposed method can detect and distinguish multiple fault events.

V. Conclusion

This paper presented an adaptive observer-based method for detecting both demagnetization and ITSC faults in PMSMs. The proposed observer estimates the d-q stator currents, permanent-magnet flux linkage, and equivalent ITSC fault-current components. Based on these estimated quantities, fault-related residuals are generated to indicate and distinguish different fault conditions. The effectiveness of the proposed method is verified through Simulink simulations. The residuals remain near zero under normal and unbalanced load torque variations. Under fault conditions, the demagnetization fault mainly increases the demagnetization residual r_{demag}, while the ITSC fault produces a clear increase in the ITSC residual r_{ITSC}. In the combined-fault case, the residuals responded sequentially to the occurrence of each fault, demonstrating the capability to detect and distinguish multiple fault events. The proposed method also maintains effective fault detection under the considered motor parameter variations. Future work will focus on experimental validation of the proposed method using a hardware PMSM drive platform. The robustness of the proposed method under practical uncertainties, including measurement noise, larger parameter mismatch, and reversible magnetic saturation, will also be investigated.

References

[1] H. Chen, J. Tang, Y. Liu, B. Jiang, and L. Boscaglia, "Electromagnetic performance investigation of a brushless electrically excited synchronous machine for long-distance heavy-duty electric vehicles," *IEEE Transactions on Transportation Electrification*, vol. 11, no. 1, pp. 225–235, 2025.

[2] C. Liao, N. Bianchi, and Z. Zhang, "Recent developments and trends in high-performance pmsm for aeronautical applications," *Energies*, vol. 17, no. 23, 2024. [Online]. Available: https://www.mdpi.com/1996-1073/17/23/6199

[3] Y. Li, R. Ma, X. Wang, J. Liang, and T. He, "Pmsm rotor position estimation via hall vector filtering phase-locked method," in *IECON 2025 – 51st Annual Conference of the IEEE Industrial Electronics Society*, 2025, pp. 1–6.

[4] S. Grubic, J. M. Aller, B. Lu, and T. G. Habetler, "A survey on testing and monitoring methods for stator insulation systems of low-voltage induction machines focusing on turn insulation problems," *IEEE Transactions on Industrial Electronics*, vol. 55, no. 12, pp. 4127–4136, 2008.

[5] M. Zafarani, E. Bostanci, Y. Qi, T. Goktas, and B. Akin, "Interturn short-circuit faults in permanent magnet synchronous machines: An extended review and comprehensive analysis," *IEEE Journal of Emerging and Selected Topics in Power Electronics*, vol. 6, no. 4, pp. 2173–2191, 2018.

[6] C.-P. Yi, P.-J. Ho, C.-J. Liu, F.-C. Lee, and S.-C. Yang, "Uniform and localized magnet demagnetization detection of permanent magnet motor based on on-line flux estimation," in *2022 IEEE Energy Conversion Congress and Exposition (ECCE)*, 2022, pp. 1–5.

[7] K.-J. Shih, M.-F. Hsieh, B.-J. Chen, and S.-F. Huang, "Machine learning for inter-turn short-circuit fault diagnosis in permanent magnet synchronous motors," *IEEE Transactions on Magnetics*, vol. 58, no. 8, pp. 1–7, 2022.

[8] F. Huang, X. Zhang, G. Qin, J. Xie, J. Peng, S. Huang, Z. Long, and Y. Tang, "Demagnetization fault diagnosis of permanent magnet synchronous motors using magnetic leakage signals," *IEEE Transactions on Industrial Informatics*, vol. 19, no. 4, pp. 6105–6116, 2023.

[9] Y. Yu, Y. Li, D. Zeng, Y. Hu, and J. Yang, "Permanent magnet synchronous motor demagnetization fault diagnosis and localization," *IEEE Sensors Journal*, vol. 25, no. 11, pp. 19 993–20 014, 2025.

[10] H. Jeong, S. Moon, and S. W. Kim, "An early stage interturn fault diagnosis of pmsms by using negative-sequence components," *IEEE Transactions on Industrial Electronics*, vol. 64, no. 7, pp. 5701–5708, 2017.

[11] Y. Rao, W. Wang, J. Fu, Z. Zheng, W. Hua, and M. Cheng, "Interturn short-circuit fault diagnosis method of pmsm servo system based on high-frequency negative sequence components," *IEEE Transactions on Power Electronics*, vol. 41, no. 2, pp. 1943–1953, 2026.

[12] R. Ortega, A. Bobtsov, L. Fang, O. Texis-Loaiza, and J. Schiffer, "Interturn fault detection in pmsms: Two adaptive observer-based noise insensitive solutions," *IEEE Transactions on Control Systems Technology*, vol. 34, no. 1, pp. 369–380, 2026.

[13] A. Belkhadir, R. Pusca, R. Romary, D. Belkhayat, and Y. Zidani, "Detection of external rotor pmsm inter-turn short circuit fault using extended kalman filter," in *2023 IEEE 14th International Symposium on Diagnostics for Electrical Machines, Power Electronics and Drives (SDEMPED)*, 2023, pp. 491–497.

[14] P. Luo, Z. Yin, Z. Zhang, Y. Zhang, P. Zhang, and J. Liu, "Diversified diagnosis strategy for pmsm inter-turn short-circuit fault via novel sliding mode observer," *IEEE Transactions on Power Electronics*, vol. 39, no. 4, pp. 4149–4159, 2024.

[15] Y. Kang and L. Yao, "Fault diagnosis for permanent magnet synchronous motor with demagnetization fault and sensor fault," *IEEE Transactions on Instrumentation and Measurement*, vol. 73, pp. 1–11, 2024.

[16] A. A. Alfehaid, E. G. Strangas, and H. K. Khalil, "Speed control of permanent magnet synchronous motor with uncertain parameters and unknown disturbance," *IEEE Transactions on Control Systems Technology*, vol. 29, no. 6, pp. 2639–2646, 2021.

[17] Y. Kang and L. Yao, "Fault isolation and estimation for turn-to-turn short circuit in permanent magnet synchronous motor," *IEEE Transactions on Instrumentation and Measurement*, vol. 73, pp. 1–11, 2024.

[18] R. Hu, J. Wang, A. R. Mills, E. Chong, and Z. Sun, "Current-residual-based stator interturn fault detection in permanent magnet machines," *IEEE Transactions on Industrial Electronics*, vol. 68, no. 1, pp. 59–69, 2021.